Characterization of erosion-like defects in multilayer porous materials

Mehdi Mohammed, Pierre Marechal, Abdellah Alem, Hervé Franklin, Huaqing Wang

17e Congrès Français d'Acoustique
27-30 avril 2025, Paris

Characterization of Erosion-Like Defects in Multilayer Porous Materials.

Mehdi Mohammed [a], Pierre Maréchal [a], Abdellah Alem [a], Hervé Franklin [a] and Huaqing Wang [a]
[a] Laboratoire Ondes et Milieux Complexes (LOMC) UMR CNRS 6294, 75 rue Bellot, Université Le Havre Normandie, Le Havre, France

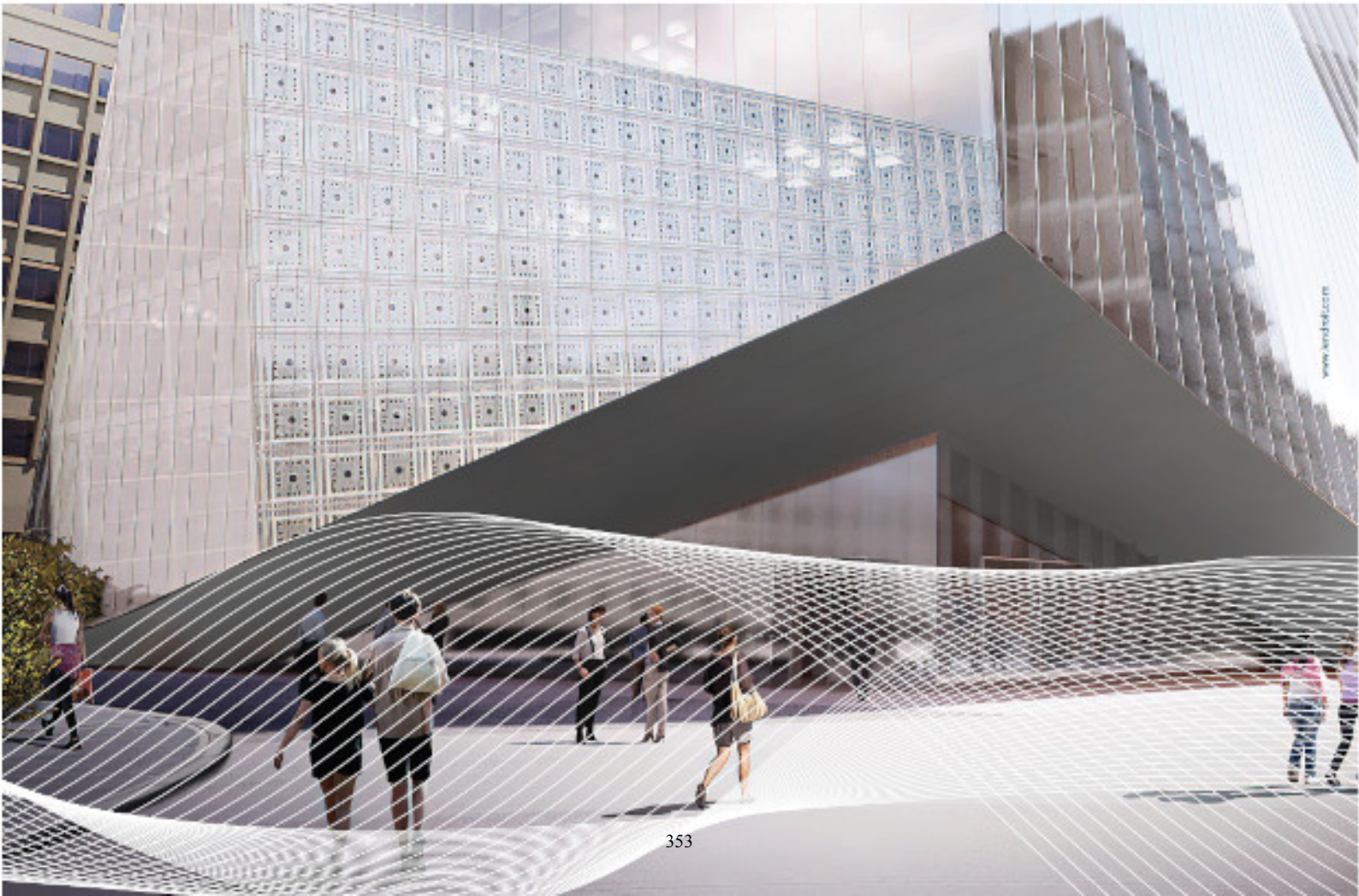

This paper study the transmission coefficient of a multilayer system consisting of two porous plates of fixed thicknesses separated by a fluid layer, and more particularly the influence of the distance between the plates on the behavior of acoustic waves. The formula for calculating the transmission coefficient of a single plate is obtained by relying on Biot's theory for porous media, which takes into account the interaction between the elastic matrix and the fluid flow inside the pores. To model the transmission coefficient of the multilayer system by keeping the formula found for the coefficient of a single plate, the Fabry-Perot method is applied. It exploits the phenomena of multiple reflection taking place in the fluid layer, and allows to control simply the variations of spacing between plates. Experimental measurements of the reflection coefficients are made for several layers of the fluid layer (0 mm, 2 mm and 4 mm). Changes in transmission behaviour are well observed when the frequency varies (from 0.1 to 1.0 MHz). Experimental results are compared with theoretical models to assess the accuracy and predictive capacity of simulations. Although the experimental coefficients of reflection are generally in line with theoretical models, there is some divergence, probably due to the complexity of the material on the one hand and the multilayer system on the other. This work offers valuable insights on the behaviour of acoustic waves in defected porous materials. It shows how variations in the spacing between media initially in contact can be detected, for example, changes in the size of a crack due to erosion under the influence of water flows in a soil. These results will provide the basis for non-destructive methods for erosion detection in porous media.

1 Introduction

Poroelastic materials, such as rocks and soils, are susceptible to fractures and cracks that can extend deep into the material, compromising its structural integrity. When these defects are filled with liquids, the mechanical properties of the material deteriorate. Detection of these defects and monitoring their expansion due to material deterioration requires a non-destructive and cost-effective method

To study erosion phenomena, a novel modeling approach is proposed, consisting of two poroelastic plates in contact. As these plates slowly separate, the controlled separation simulates the progressive formation of defects caused by erosion. This process conceptually replicate the transition from full contact with no erosion to gaps of varying sizes. The setup models a defect within an isotropic poroelastic medium, simplified by assuming it separates two plates with thicknesses of $2h^{(a)}$ and $2h^{(b)}$, both significantly thicker than the defect itself, which has a thickness e. The primary objective of the study is to explore how acoustic waves can be used to detect the development of such defects.

Both the plates and the defect are considered infinite in the x-y plane but finite along the z-axis, as illustrated in Figure 1. The system is immersed in a fluid-filled environment, and we adopt Biot's theory of fluid-saturated poroelastic media, accounting for deformations in the skeleton of the material and the interaction between the skeletal structure and the saturating fluid.

Biot's theory [1] predicts three types of wave modes in a porous medium: two longitudinal waves (fast compressional wave and slow compressional wave - indexed as 1 and 2, respectively) and a transverse shear wave (denoted as t). The fast compressional wave involves the motion of the solid and fluid in phase, similar to a classical elastic wave, while the slow compressional wave is dominated by relative motion between the solid and the pore fluid, leading to significant attenuation. The shear wave propagates through the solid matrix and is largely unaffected by the pore fluid.

The propagation speeds of these waves are influenced by factors such as porosity, permeability, and the bulk moduli of the constituents. The fluid phase modifies the wave attenuation and dispersion characteristics due to viscoelastic and inertial coupling effects. Experimental observations by Plona [2] have shown the slow wave in porous plates, especially at interfaces where the fluid can move freely through open pores. When a plane wave is incident in oblique angle, all three types of wave are generated through mode conversion. However, at normal incidence, only the fast and slow waves can propagate. Studies by Rasolofosaon [3] suggest that the slow wave does not transmit when the plate faces have closed pores, regardless of the incidence angle.

In this work, we focus specifically on plates with open pores, using QF20 material from Filtros® Ferro Corporation for the experimental setup due to its well-documented mechanical and acoustic properties, as noted in Johnson's work [4].

2 Theoretical basis

A poroelastic medium consists of two connected phases: a solid skeleton and a fluid that saturates the pore space. The solid phase has a mass density ρ_s and bulk modulus K_s, while the fluid phase has a mass density ρ_0 and sound velocity c_0. The porosity β represents the fraction of the total volume occupied by the fluid. The effective mass density of the medium is $\rho = (1-\beta)\rho_s + \beta\rho_0$. The displacement fields of the system are defined as $\mathbf{u}$ for the solid matrix and $\mathbf{U}$ for the pore fluid. The relative displacement of the fluid with respect to the solid is $\mathbf{w} = \beta(\mathbf{U}-\mathbf{u})$. The local increase in fluid content, representing the volumetric flow of the pore fluid, is $\zeta = -\nabla \cdot \mathbf{w}$. For a homogeneous and isotropic poroelastic medium, the strain tensor is defined as: $\bar{\bar{\epsilon}} = \frac{1}{2}(\nabla\mathbf{u} + \nabla\mathbf{u}^T)$ and the volumetric strain of the solid skeleton is $\epsilon_I = \mathrm{tr}(\bar{\bar{\epsilon}}) = \nabla\cdot\mathbf{u}$. The constitutive relations for the stress tensor $\bar{\tau}$ and the pore fluid pressure P_f are given by:

$$\bar{\bar{\tau}} = 2\mu\bar{\bar{\epsilon}} + [(H-2\mu)\epsilon_I - C\zeta]\bar{\bar{I}}, \tag{1}$$

$$P_f = M\zeta - C\epsilon_I. \tag{2}$$

where ∇ is the gradient operator, $\bar{\bar{I}}$ the unit tensor and $\zeta = -\nabla.w$ is the increment of fluid content. The constant, μ is the shear modulus, and H, M, and C are poroelastic moduli that characterize the mechanical behavior of the medium. Further details can be found in Appendix A and in Refs. [5, 6, 7].

Biot [6] derived wave equations for longitudinal and transverse waves in poroelastic media from the constitutive relations, fluid flow equations, and equations of motion. Assuming harmonic wave propagation ($e^{i(\ell\bar{x}-\omega t)}$) along the horizontal z-axis, where ω is the angular frequency, t is time, and $\ell = \ell_r + i\ell_i$ is the complex wave number, where $(l_r, l_i) \in \mathbb{R}^2$, the dispersion relations are given by:

$$\begin{vmatrix} H\ell^2 - \rho\omega^2 & C\ell^2 - \rho_0\omega^2 \\ C\ell^2 - \rho_0\omega^2 & M\ell^2 - \tilde{\alpha}(\rho_0/\beta)\omega^2 \end{vmatrix} = 0, \tag{3}$$

for longitudinal waves, and

$$\begin{vmatrix} \mu\ell^2 - \rho\omega^2 & -\rho_0\omega^2 \\ \rho_0\omega^2 & \tilde{\alpha}(\rho_0/\beta)\omega^2 \end{vmatrix} = 0, \tag{4}$$

for transverse waves[9].

In these equations, $\tilde{\alpha} = \alpha + i\frac{\eta\beta}{\omega\kappa\rho_0}F$, where $\tilde{\alpha}$ is the dynamic tortuosity. The Biot complex correction factor $F = F(\chi)$, where $\chi = a_p(\omega\rho_0/\eta)^{1/2}$ (a_p being the pore size parameter), accounts for deviations from Poiseuille-type flow at higher frequencies. At low frequencies, $F(\chi) = 1$ and a_p disappear, simplifying the equations. Equation (3) has two roots: ℓ_1 corresponds to the fast wave with moderate attenuation, while ℓ_2 represents the slow wave with strong attenuation. Equation (4) has a unique root ℓ_t which correspond to transverse wave.

3 Transmission coefficient

The reflection and transmission of waves at boundaries between different media depend on the impedance differences. In a poroelastic medium, the acoustic impedance is a function of the wave modes involved. The interaction of waves at an interface leads to the generation of reflected and transmitted waves, whose amplitudes are governed by boundary conditions enforcing stress and displacement continuity. Biot's theory provides a fundamental description of wave propagation in porous media, allowing the derivation of transmission coefficients by solving the wave equations with the imposed interface conditions.

3.1 One plate

In order to investigate the elongated defect model more deeply within the context of a two-plate system, we begin by considering a single poroelastic plate, denoted by p, with a thickness $2h^{(p)}$, placed in a fluid medium. This fluid is the same fluid that saturates the pores of the plate. The boundary conditions on the plate's faces adhere to open-pore conditions, which allow unrestricted flow of the saturating fluid, thereby enabling energy exchange between the plate and the surrounding fluid.

Let us consider a harmonic plane wave with the general form $e^{i(k_x x + k_{0z} z - \omega t)}$. The plane wave is incident on the plate at the face located at $z = -h^{(p)}$, at an angle θ relative to the normal direction to the plate's surface. In this setup, the wave vectors are related by $k_x = k_0 \sin\theta$ and $k_{0z} = k_0 \cos\theta = \sqrt{k_0^2 - k_x^2}$, where $k_0 = \frac{\omega}{c_0}$ is the wave number in the surrounding fluid.

When the incident wave strikes the plate, it generates multiple wave components. Specifically, the incident wave splits into a reflected wave on the same side of the plate and a transmitted wave that propagates into the plate. Upon entering the poroelastic material, the incident wave is transformed into three distinct dispersive and attenuated waves: fast, slow, and shear waves. These waves then propagate through the plate and emerge on the opposite side as a longitudinal wave, similar to the incident wave but attenuated and potentially changed in its phase and amplitude.

The reflection $\mathcal{R}^{(p)}$ and transmission $\mathcal{T}^{(p)}$ coefficients for such a system have been extensively studied and can be found in Refs. [8]. The expressions are provided in the Appendix (see Eq. (A.1)).

3.2 System of two poroelastic plates

Now, moving to a more complex system consisting of two poroelastic plates, (a) and (b), each with thicknesses $2h^{(a)}$ and $2h^{(b)}$, respectively. These plates are separated by a fluid layer of thickness e, as depicted in Figure 1.

When a harmonic plane wave from the external fluid, located in the region $z < 0$, meets the plate (a) at an angle θ, it generates a reflected wave in the same region $z < 0$. The reflection coefficient for this wave is denoted $r^{(ab)}$. In addition to the reflected wave, part of the incident energy passes through plate (a), enters the fluid layer, and then traverses plate (b). The transmitted wave, emerging on the opposite side of plate (b) (in the region $z > 0$), has a transmission coefficient $t^{(ab)}$.

To determine the reflection and transmission coefficients for this system of two plates, we apply the well-established Fabry-Pérot method from optics [10], which takes advantage of the fact that in any finite layer, incoming waves undergo multiple reflections and transmissions as they travel through. This method assumes that the plates are coupled via multiple interactions within the fluid layer. By treating the system as a series of partial reflections and transmissions, the overall reflection and transmission coefficients for the system can be computed using the geometric series expansion.

After performing the necessary series transformations, the final reflection and transmission coefficients for the two-plate system are found to be:

$$r^{(ab)} = \mathcal{R}^{(a)} + \frac{\mathcal{T}^{(a)2}\mathcal{R}^{(b)}e^{-2i\phi}}{1 - \mathcal{R}^{(a)}\mathcal{R}^{(b)}e^{-2i\phi}}, \quad t^{(ab)} = \frac{\mathcal{T}^{(a)}\mathcal{T}^{(b)}e^{-i\phi}}{1 - \mathcal{R}^{(a)}\mathcal{R}^{(b)}e^{-2i\phi}}, \tag{5}$$

where $\phi = \ell_0 e \cos\theta$ represents the phase difference accumulated due to the wave traveling through the fluid layer of thickness e.

In the special case where plates a and b are identical as in the case of this study, such that $\mathcal{R}^{(a)} = \mathcal{R}^{(b)}$ and $\mathcal{T}^{(a)} = \mathcal{T}^{(b)}$, we obtain the following simplified expressions for the reflection and transmission coefficients:

$$r^{(aa)} = \mathcal{R}^{(a)} + \frac{\mathcal{T}^{(a)2}\mathcal{R}^{(a)}e^{-2i\phi}}{1-\mathcal{R}^{(a)2}e^{-2i\phi}}, \quad t^{(aa)} = \frac{\mathcal{T}^{(a)2}e^{-i\phi}}{1-\mathcal{R}^{(a)2}e^{-2i\phi}}. \quad (6)$$

Given that the fast, slow and shear waves propagating through the poroelastic medium experience significant attenuation due to the viscosity of the saturating fluid, the energy conservation law is not satisfied. This results in the following conditions for energy balance:

$$|\mathcal{R}^{(j)}|^2 + |\mathcal{T}^{(j)}|^2 < 1 \quad \text{for} \quad j = a, b, \quad (7)$$

and for the system of two plates:

$$|r^{(ab)}|^2 + |t^{(ab)}|^2 < 1 \quad \text{or} \quad |r^{(ba)}|^2 + |t^{(ba)}|^2 < 1. \quad (8)$$

Table 1: QF-20® and saturating fluid (water) parameters [12].

Parameter	Value
Solid bulk modulus K_s (Pa)	3.66×10^{10}
Saturating fluid bulk modulus K_f (Pa)	2.22×10^{9}
Dried frame bulk modulus K_b (Pa)	9.47×10^{9}
Dried frame shear modulus μ (Pa)	7.63×10^{9}
Saturating fluid viscosity η (Pa s)	1.14×10^{3}
Solid density ρ_s (kg/m^3)	2760
Saturating fluid density ρ_0 (kg/m^3)	1000
Porosity β	0.402
Permeability k (m^2)	1×10^{-11}
Pore radius a_p (m)	3.26×10^{-5}
Tortuosity α	1.89

4 Methodology

4.1 Experimental setup

The experimental setup aims to capture the acoustic signals of a porous QF20®plate (measuring 300 mm x 200 mm x 5.18 mm) submerged vertically in water. Two non-focused Panametrics® transducers, each with a central frequency of 0.5 MHz and an active diameter of 1.5 inch, are employed for the measurements. Positioned 15 cm apart, these transducers operate under the assumption of negligible diffraction and utilize a plane wave model.

The experimental setup is shown in Figure 2 and the procedure begins with calibrating the transducers. Initially, they are aligned face-to-face without the plate present. Once calibrated, the plates are introduced, and adjustments ensure the plates sit perpendicular to the transducers (normal incidence). Subsequently, fine-tuning of the transducers in order to maximize the peak value of the transmitted signal.

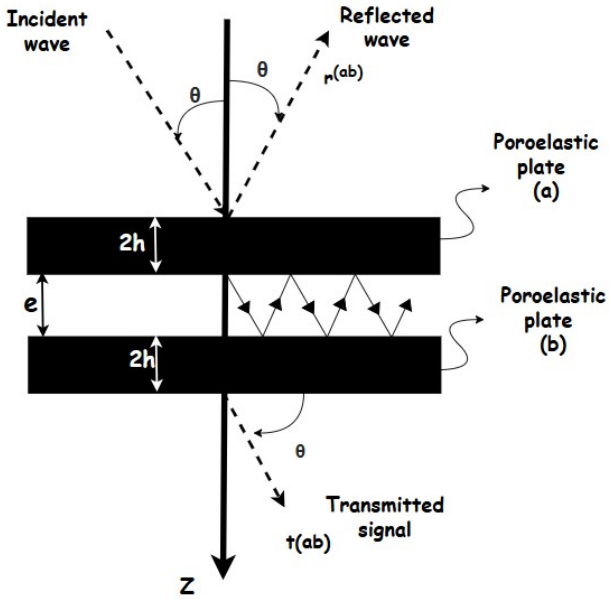

Figure 1: Reflection and transmission of waves by a system of two porous plates saturated with fluid and immersed in an infinite fluid. Waves passing through the first poroelastic layer (a) penetrate the defect. They then undergo an infinite number of reflections and partial transmissions between the opposite faces of layers (a) and (b). These partial waves contribute to the overall reflection on the face of layer (a) and to the overall transmission on the face of layer (b)

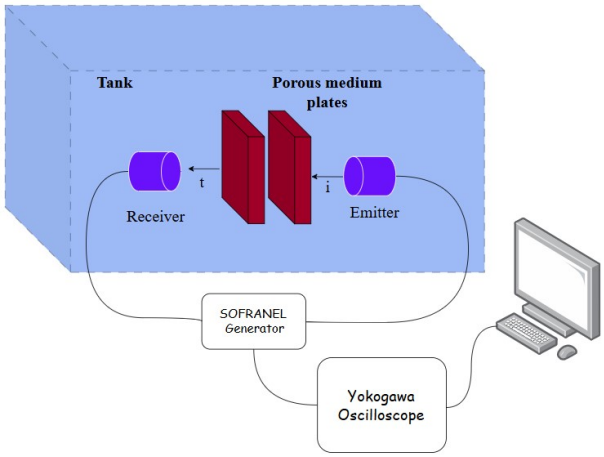

Figure 2: Experimental setup.

After the first measurement, where the two plates are in contact with a 0 mm distance, subsequent tests are conducted by gradually increasing the distance between the plates to 2 mm and finally 4 mm. Each test is followed by calibration to ensure optimal alignment and signal accuracy for each separation.

The experimental transmission coefficient is then computed by applying a Fast Fourier Transform to the received transmitted signal. This transmitted signal data is analyzed and compared to theoretical model that is

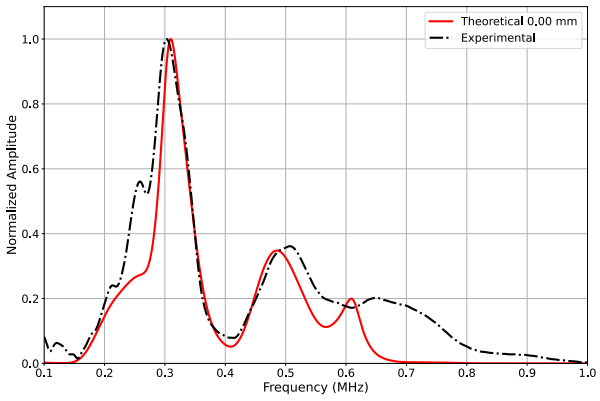

Figure 3: Transmission coefficient of an acoustic wave with a water layer thickness of 0 mm, theoretically and experimentally.

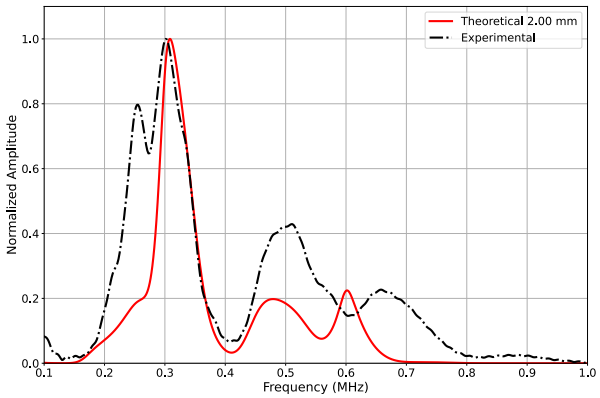

Figure 4: Transmission coefficient of an acoustic wave with a water layer thickness of 2 mm, theoretically and experimentally.

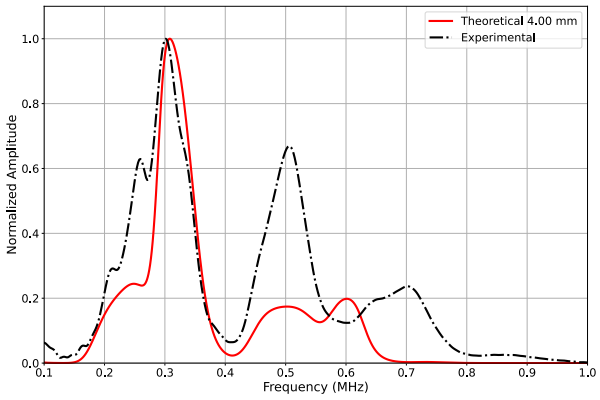

Figure 5: Transmission coefficient of an acoustic wave with a water layer thickness of 4 mm, theoretically and experimentally

developed in section 2, allowing for the extraction of relevant material properties of the plate. Following signal processing, a manual adjustment is implemented to minimize the discrepancy between experimental and theoretical transmission coefficients. Biot parameters such as permeability and tortuosity are manually fine-tuned to achieve the best alignment between theoretical model and experimental data. The exact value of QF20 used for theoretical modelling is listed in Table 1, which is based on previous studies conducted on the same material. [8][12].

4.2 Signal treatment

To compare the theoretical results with the experimental data, adjustments are made to account for the frequency response characteristics of the transducer used in the measurements. The first step involves modifying the theoretical transmission coefficient by multiplying it with a Gaussian function [11]. This adjustment effectively adopt the the coefficient to match the finite bandwidth of the transducer, ensuring a good comparison between theory and experiment that considers the limitations of the experimental setup.

The Gaussian function models the transducer's behavior by adjusting the central frequency and variance, allowing the theoretical transmission coefficient to more accurately reflect the transducer's performance. For the experimental data, the Fast Fourier Transform (FFT) is applied to convert the time-domain signal into the frequency domain. After normalizing both signals, the adjusted theoretical transmission coefficients are compared with the experimental results as shown in Figures 3, 4 and 5.

5 Discussion

Figures 3 to 5 compare the experimental and theoretical transmission spectra for two porous plates separated by water layers of thicknesses 0mm (in contact), 2mm and 4mm. The experimental data (dashed curves) exhibit distinct resonance peaks around 0.3 MHz and 0.50 MHz, broadly matching the predictions of the Biot-based theoretical model (solid curves). This general correspondence confirms that Biot's theory can capture the principal wave modes—both in terms of resonance frequency and qualitative amplitude behavior—when dealing with porous plates immersed in water.

Despite this good overall agreement, some notable discrepancies are evident. First, the main resonance peak at approximately 0.3MHz is sharper and slightly higher in amplitude in the experimental data than in the model. Increasing the plate thickness by 5–10% in the simulation yields a closer match, highlighting the strong sensitivity of resonance to small changes in thickness. Given the porous and rough surfaces of the plates, it is reasonable that the "effective" acoustic thickness is larger than the mechanically measured 5.18mm

A second factor is the presence of thin fluid layer. Even at "0mm" separation, rough surfaces and imperfect contact almost certainly admit a very thin layer of water between the plates. This changes the boundary conditions in ways not fully captured by a simple model of perfect

contact. For the remaining tests, introducing a water gap modifies the interference pattern, resulting in shifts of some secondary peaks, while the primary resonance remains largely unaffected. These changes are broadly mirrored in the theoretical curves

Material-property uncertainties can also affect the amplitude in the model. In Biot theory, parameters such as porosity, tortuosity, frame modulus, and frequency-dependent attenuation all influence wave propagation in porous media. If any of these values differ from nominal or are not measured with sufficient precision, discrepancies may appear in both peaks and minima location. In particular, frequency-dependent attenuation mechanisms in porous media can cause broader or shallower peaks than predicted by simplified damping models.

In summary, the measured and modeled data show qualitatively close resonance structures for all water layer thicknesses configurations, supporting the validity of a Biot-based approach. However, small deviations in effective plate thickness, unmodeled thin water layer at the interfaces, and uncertainties in material parameters likely contribute to the observed quantitative differences.

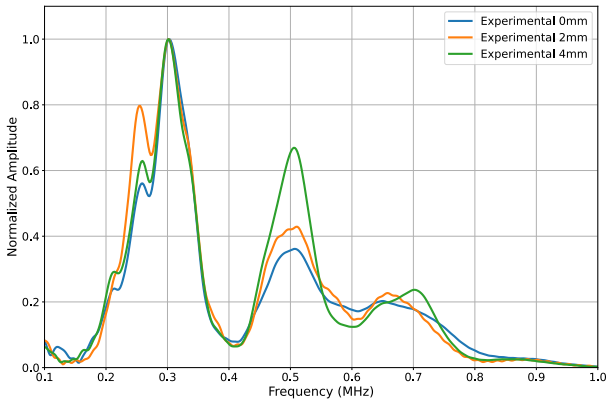

Figure 6: Superimposed experimental results.

The experimental results presented in Figure 6 reveal a notable trend: as the thickness of the water layer increases, there is a clear increment in the signal amplitude at approximately 0.5 MHz. This frequency aligns with the transducer's center frequency, which may contribute to the enhanced accuracy and clarity of the measurements at this point. At 0.5 MHz, the amplitude is highest for the 4 mm thickness and lowest for the 0 mm thickness, suggesting that thicker water layers enhance the signal amplitude.

However, at the lower frequency of around 0.25 MHz, the pattern is less clear. While the 4 mm thickness shows a relatively high amplitude, the differences among the various thicknesses are not as pronounced or consistent. This lack of clarity might be due to the transducer's reduced sensitivity away from its center frequency.

The third peak, around 0.7 MHz, is less prominent compared to the first two peaks, and the differences in amplitudes among the setups are small. Nevertheless, the general trend of increasing amplitude with thickness is still observable.

This observation is important as it suggests that water thickness can be estimated from the frequency response of the system, particularly at the transducer's center frequency of approximately 0.5 MHz.

6 Conclusion

This paper studies the transmission of acoustic wave of a multilayer system consisting of two poroelastic plates separated by a fluid layer. The objective of the study was to observe the influence of the variation of the distance between the plates on the acoustic wave signals. Theoretical model have been developed in order to calculate the transmission coefficient of the two plates. Experimental measurements of the transmission coefficients are conducted for several thicknesses of the fluid layer (0 mm, 2 mm, and 4 mm). Changes in transmission behavior are well observed as the frequency varies from 0.1 to 1.0 MHz. Notably, the results show a clear increment in signal amplitude at approximately 0.5 MHz with increasing fluid layer thickness. However, the pattern at lower frequencies is less clear. Experimental results are compared with theoretical models to assess the accuracy and predictive capacity of the simulations. Although the experimental coefficients of reflection are generally in line with theoretical models, some divergence is observed, likely due to the complexity of the material and the multilayer system.

Future work should focus on improving the method for assessing erosion detection. Rather than increasing the distance between the plates, it may be more representative to decrease the thickness of the plate or the material to simulate the eroded part.

Appendix A : Reflection and transmission coefficients

The reflection and transmission coefficients of a fluid-saturated porous plate with open pore conditions at the boundaries are given by [8]

$$\mathcal{R}^{(j)} = \frac{1}{2}\left(\frac{\delta_S^{(j)}}{\bar{\delta}_S^{(j)}} + \frac{\delta_A^{(j)}}{\bar{\delta}_A^{(j)}}\right), \quad \mathcal{T}^{(j)} = \frac{1}{2}\left(\frac{\delta_S^{(j)}}{\bar{\delta}_S^{(j)}} - \frac{\delta_A^{(j)}}{\bar{\delta}_A^{(j)}}\right) \tag{A.1}$$

$$\begin{aligned}
\delta_A^{(j)} &= C_{AF1}^{(j)}C_{A2}^{(j)} - C_{AF2}^{(j)}C_{A1}^{(j)} - i\tau_2\left(C_{AF1}^{(j)} - C_{A1}^{(j)}\right) + i\tau_1\left(C_{AF2}^{(j)} - C_{A2}^{(j)}\right),\\
\bar{\delta}_A^{(j)} &= C_{AF1}^{(j)}C_{A2}^{(j)} - C_{AF2}^{(j)}C_{A1}^{(j)} + i\tau_2\left(C_{AF1}^{(j)} - C_{A1}^{(j)}\right) - i\tau_1\left(C_{AF2}^{(j)} - C_{A2}^{(j)}\right),\\
\delta_S^{(j)} &= C_{SF1}^{(j)}C_{S2}^{(j)} - C_{SF2}^{(j)}C_{S1}^{(j)} + i\tau_2\left(C_{SF1}^{(j)} - C_{S1}^{(j)}\right) - i\tau_1\left(C_{SF2}^{(j)} - C_{S2}^{(j)}\right),\\
\bar{\delta}_S^{(j)} &= C_{SF1}^{(j)}C_{S2}^{(j)} - C_{SF2}^{(j)}C_{S1}^{(j)} - i\tau_2\left(C_{SF1}^{(j)} - C_{S1}^{(j)}\right) + i\tau_1\left(C_{SF2}^{(j)} - C_{S2}^{(j)}\right),
\end{aligned} \tag{A.2}$$

In Eqs. (A.2),

$$\begin{aligned}
C_{AFp}^{(j)} &= P_p \tan\left(k_{pz}h^{(j)}\right),\\
C_{SFp}^{(j)} &= P_p \cot\left(k_{pz}h^{(j)}\right),\\
C_{Ap}^{(j)} &= M_p \tan\left(k_{tz}h^{(j)}\right) + N_p \tan\left(k_{pz}h^{(j)}\right),\\
C_{Sp}^{(j)} &= M_p \cot\left(k_{tz}h^{(j)}\right) + N_p \cot\left(k_{pz}h^{(j)}\right),\\
\tau_p &= \frac{\rho_0}{\rho}\ell_t^2\frac{k_{pz}}{k_{0z}}\left[(1+\gamma_p)(\ell_t^2 - 2k_x^2) + 2k_x^2(1+\gamma_t)\right],
\end{aligned} \tag{A.3}$$

where

$$\begin{aligned}
P_p &= \tfrac{\rho_{fp}}{\rho_t}\ell_t^2(\ell_t^2 - 2k_x^2),\\
M_p &= 4k_x^2 k_{tz}k_{pz},\\
N_p &= \left(\tfrac{\rho_p}{\rho_t}\ell_t^2 - 2k_x^2\right)(\ell_t^2 - 2k_x^2)
\end{aligned} \tag{A.4}$$

It is recalled that above the indices $p = 1$ and $p = 2$ refer to the fast and slow waves, respectively. Note that $k_{pz} = (\ell_p^2 - k_x^2)^{\frac{1}{2}}$ and $k_{tz} = (\ell_t^2 - k_x^2)^{\frac{1}{2}}$, where ℓ_p and ℓ_t define the wavenumbers relative to longitudinal and shear waves in the porous medium. The subscripts A (for antisymmetric) and S (for symmetric) refer to the two possible vibration modes of a free plate. The quantities ρ_p, ρ_{fp} and ρ_t have the dimensions of a mass density. The coefficients γ_p and γ_t are dimensionless. They are given by [8] :

$$\gamma_p = \frac{H\ell_p^2 - \rho\omega^2}{\rho_f\omega^2 - C\ell_p^2} \quad (p = 1, 2), \tag{A.5}$$

$$\gamma_t = \frac{\mu\ell_t^2 - \rho\omega^2}{\rho_f\omega^2}. \tag{A.6}$$

$$\rho_p = \left(H + \gamma_p C\right)\frac{\ell_p^2}{\omega^2} \quad (p = 1, 2), \tag{A.7}$$

$$\rho_{fp} = \left(C + \gamma_p M\right)\frac{\ell_p^2}{\omega^2} \quad (p = 1, 2), \tag{A.8}$$

$$\rho_t = \mu\frac{\ell_t^2}{\omega^2}. \tag{A.9}$$

Above, and in section 2 the constants H, M, C introduced depend on several parameters of the porous medium, *cf.* [5], [7] :

$$H = \frac{(K_s - K_b)^2}{D - K_b} + K_b + \frac{4}{3}\mu, \quad M = \frac{{K_s}^2}{D - K_b}. \tag{A.10}$$

$$C = \frac{K_s(K_s - K_b)}{D - K_b}, \quad D = K_s\left[1 + \beta\left(\frac{K_s}{K_f} - 1\right)\right]. \tag{A.11}$$

References

[1] Biot M. A. , Theory of propagation of elastic waves in a fluid-saturated porous solid, I. Low-frequency range, J. Acoust. Soc. Am. 28 (2) (1956) 168 –178

[2] Plona T. J., Observation of a second bulk compressional wave in a porous medium at ultrasonic frequencies, Appl. Phys. Lett. 36 (4) (1980), 259-261

[3] Rasolofosaon P., Impotance of the interface hydraulic condition on the generation of second bulk compressional wave in porous media, Appl. Phys. Lett., 52 (1988) pp 780-782.

[4] Johnson D. L., Plona T. J., Kojima H., Probing porous media with first and second sound: II acoustic properties of water saturated porous media, J. Appl. Phys 76 (1) (1994), 115-125.

[5] R.D. Stoll, T.-K. Kan Reflection of acoustic waves at a water-sediment interface, J. Acoust. Soc. Am. 70 (1) (1981), 149-156.

[6] M. A. Biot, D. G. Willis, The elastic coefficients of the theory of consolidation, J. Appl. Mech. 24 (1957), 594.

[7] J. G. Berryman, Elastic wave propagation in fluid-saturated porous media, J. Acoust. Soc. Am. 69 (2) (1981), 416-424.

[8] G. Belloncle, H. Franklin, F. Luppé, and J. M. Conoir, Normal modes of a poroelastic plate and their relation to the reflection and transmission coefficients, Ultrasonics 41 (2003), 207–216.

[9] Belloncle, G., Luppé, F., *Ondes guidées dans une plaque poroélastique immergée dans l'eau*, Thèse de doctorat, Université du Havre, 2002. Available: https://www.sudoc.fr/069416400.

[10] M. Born, E. Wolf *Principles of Optics: Electromagnetic Theory of Propagation, Interference and Diffraction of Light*, 7th (expanded) edition, Cambridge University Press, 13 oct. 1999 - 952 pages ISBN 0521642221, 9780521642224

[11] P. Manoochehrnia, P. Maréchal , D. Leduc and M. E. El-Kettani, Inverse Problem-Solving Method Applied to the Acoustic Characterisation of a Thin Film via the Debye Series Method (DSM). Nondestructive Testing and Evaluation, 21 Oct. 2024, pp. 1–23, https://doi.org/10.1080/10589759.2024.2411003.

[12] Franklin, H., Derible, S., Popa, C., Expansions of reflected-transmitted signals to estimate the slow wave strength in fluid-saturated porous layers, J. Appl. Phys., vol. 108, no. 5, p. 054907, 2010. DOI: 10.1063/1.3479705.